Focal and segmental glomerulosclerosis induced in mice lacking decay-accelerating factor in T cells

Lihua Bao,[1] Mark Haas,[2] Jeffrey Pippin,[3] Ying Wang,[1] Takashi Miwa,[4] Anthony Chang,[5] Andrew W. Minto,[1] Miglena Petkova,[1] Guilin Qiao,[1] Wen-Chao Song,[4] Charles E. Alpers,[6] Jian Zhang,[1] Stuart J. Shankland,[3] and Richard J. Quigg[1]

[1]Section of Nephrology, University of Chicago, Chicago, Illinois, USA. [2]Department of Pathology, Johns Hopkins University School of Medicine, Baltimore, Maryland, USA. [3]Division of Nephrology, University of Washington School of Medicine, Seattle, Washington, USA. [4]Institute for Translational Medicine and Therapeutics and Department of Pharmacology, University of Pennsylvania School of Medicine, Philadelphia, Pennsylvania, USA. [5]Department of Pathology, University of Chicago, Chicago, Illinois, USA. [6]Department of Pathology, University of Washington School of Medicine, Seattle, Washington, USA.

Heritable and acquired diseases of podocytes can result in focal and segmental glomerulosclerosis (FSGS). We modeled FSGS by passively transferring mouse podocyte–specific sheep Abs into BALB/c mice. BALB/c mice deficient in the key complement regulator, decay-accelerating factor (DAF), but not WT or CD59-deficient BALB/c mice developed histological and ultrastructural features of FSGS, marked albuminuria, periglomerular monocytic and T cell inflammation, and enhanced T cell reactivity to sheep IgG. All of these findings, which are characteristic of FSGS, were substantially reduced by depleting $CD4^+$ T cells from $Daf^{-/-}$ mice. Furthermore, WT kidneys transplanted into $Daf^{-/-}$ recipients and kidneys of DAF-sufficient but T cell–deficient $Balb/c^{nu/nu}$ mice reconstituted with $Daf^{-/-}$ T cells developed FSGS. In contrast, DAF-deficient kidneys in WT hosts and $Balb/c^{nu/nu}$ mice reconstituted with DAF-sufficient T cells did not develop FSGS. Thus, we have described what we believe to be a novel mouse model of FSGS attributable to DAF-deficient T cell immune responses. These findings add to growing evidence that complement-derived signals shape T cell responses, since T cells that recognize sheep Abs bound to podocytes can lead to cellular injury and development of FSGS.

Introduction

The complement system is the first line of defense against some microorganisms and an integral component of innate and adaptive immune responses to many others. Complement proteins are also important for clearing immune complexes and material derived from apoptotic cells; in so doing, they can shape the immune response to diverse antigens, including those from self and allogeneic tissue (1–3). Activation through classical, alternative, or lectin complement pathways leads to the cleavage of C3 and C5 and generation of C3a, C3b, C5a, and C5b. The receptors for C3a and C5a are 7-span transmembrane G protein–coupled receptors of the rhodopsin family, while C3b-binding proteins are in the regulators of complement activation and β_2 integrin families. In the former is decay-accelerating factor (DAF, also known as CD55), which is encoded by 1 gene in humans and 2 in mice, in which the *Daf1* product has the most relevance to human DAF (4). DAF is important for restricting complement activation on selected cells, such as on the erythrocyte in paroxysmal nocturnal hemoglobinuria and locally on podocytes in nephrotoxic serum nephritis (5–7). Yet an increasing repertoire of actions has been shown for DAF, such as its serving as the receptor for *Helicobacter pylori* (8) and leading to tyrosine kinase-mediated cellular activation when cross-linked on the surface of T cells (9, 10). While C3b is a natural ligand for DAF, it has low binding affinity, which has led to an active search for other potential ligands, such as the 7-span transmembrane protein CD97 (11, 12). The possibility that DAF can also modulate T cell function in vivo has been supported by studies in $Daf^{-/-}$ mice (13, 14).

Though there are various inherited disorders of the podocyte, the majority of podocyte diseases are acquired and largely unexplained (15). Focal and segmental glomerulosclerosis (FSGS) is a common and unfavorable sequel to severe podocyte injury. The characteristic ultrastructural finding in FSGS, as is also true of the often-related minimal change disease, is diffuse effacement of podocyte foot processes. It has been proposed that minimal change disease (and selected cases of FSGS) reflects a disorder of T cells, potentially through the release of cytokines, including a still unidentified "permeability factor" (16). Considerable investment has been made in developing rodent models of minimal change disease/FSGS, including through hemodynamic and toxic podocyte stressors. We passively administered heterologous anti-podocyte Abs into mice, with the expectation that host humoral immune response would amplify injury to the targeted podocytes. In BALB/c mice, DAF-deficient T cells mounted an immune response to the local podocyte-bound heterologous IgG, resulting in clinical and pathological features of human FSGS.

Results

Initial characterization of anti-podocyte antibody. We generated sheep Abs to early passage–cultured mouse podocytes, with the intention of inducing Ab-dependent podocyte pathology; based on

Authorship note: Mark Haas, Jeffrey Pippin, and Ying Wang contributed equally to this work.

Conflict of interest: The authors have declared that no conflict of interest exists.

Nonstandard abbreviations used: anti-podo, sheep anti-mouse podocyte; DAF, decay-accelerating factor; FSGS, focal and segmental glomerulosclerosis; hpf, high-power field.

Citation for this article: *J. Clin. Invest.* **119**:1264–1274 (2009). doi:10.1172/JCI36000.

our past studies with rat podocytes, we anticipated disease features comparable to those of anti-Fx1A–induced membranous nephropathy (Heymann nephritis) (17). Here, we concentrated on a sheep anti-mouse podocyte (anti-podo) Ab preparation reactive with a limited set of glomerular antigens that were distinct from those identified by nephrotoxic serum and anti-Fx1A, most notably type IV collagen and megalin; moreover, its reactivities were distinct from those of other Abs generated in sheep to cultured mouse podocytes (Supplemental Figure 1; supplemental material available online with this article; doi:10.1172/JCI36000DS1). Upon passive administration to mice, immunofluorescence microscopy revealed sheep IgG and mouse C3 bound to the glomerular capillary wall in a relatively linear pattern. Ultrastructurally, passively transferred anti-podo Abs bound to both apical and basal domains of the podocyte surface and also were evident in intracellular podocyte vesicular structures (Supplemental Figure 2).

In subsequent experiments in which normal C57BL/6 mice were passively administered varying doses of anti-podo Abs, sheep IgG and mouse C3 were identified bound to the glomerular capillary wall. In the subsequent autologous phase, mouse IgG was also evident within the glomerular capillary wall, consistent with the generation of an immune response to the heterologous sheep IgG. Yet in no instance was there development of glomerular disease, as shown histologically or by increased albuminuria (data not shown). To enhance the likelihood of productive disease, we subsequently studied C57BL/6 mice lacking DAF and/or CD59, with the rationale that these are the major complement regulatory proteins of mouse and human podocytes (5, 6, 18, 19). Yet, as in WT C57BL/6 mice, in no instance did anti-podo Abs lead to glomerular disease features of any kind (data not shown).

To evaluate whether background strain might underlie the lack of disease features in C57BL/6 mice, we subsequently studied *Daf*$^{-/-}$*Cd59*$^{-/-}$ BALB/c mice (≥ N10). Here, our rationale was that the BALB/c strain is relatively skewed toward Th2 immune responses, including in glomerular diseases (20, 21), which contrasts with the Th1 response in C57BL/6 mice. In these experiments, *Daf*$^{-/-}$*Cd59*$^{-/-}$ mice developed albuminuria, which increased progressively over time following injection and was dependent on the quantity of anti-podo Abs. Thirty days after injection of 0, 0.17, 0.33, and 0.67 mg/g body weight anti-podo IgG, urinary albumin was 0.03 ± 0.00, 0.3 ± 0.2, 75.0 ± 28.5, and 163.4 ± 25.6 mg/mg creatinine, respectively. Thus, passively administered anti-podo Abs leads to massive albuminuria in *Daf*$^{-/-}$*Cd59*$^{-/-}$ mice on a BALB/c genetic background.

Anti-podo Ab–induced FSGS. Further experiments were performed to dissect anti-podo Ab–induced dose-dependent albuminuria in *Daf*$^{-/-}$*Cd59*$^{-/-}$ BALB/c mice. The requirements for DAF and/or CD59 deficiencies were first evaluated. While WT and *Cd59*$^{-/-}$ mice developed relatively mild albuminuria, *Daf*$^{-/-}$ and *Daf*$^{-/-}$*Cd59*$^{-/-}$ mice had markedly increased albuminuria 30 days following a single injection of 0.67 mg/g body weight anti-podo IgG (Figure 1A) ($P < 0.001$). These were not different from each other but were significantly different from values from WT and *Cd59*$^{-/-}$ mice, confirming that disease was attributable to DAF deficiency.

In glomeruli of all mice, there was prominent glomerular capillary wall deposition of mouse IgG and somewhat lesser quantities of sheep IgG, reflecting the remaining bound anti-podo Abs (Figure 1B). There was also segmental and discontinuous C3 deposition in glomeruli from all animals. Consistent with the lack of C3 convertase regulation from absent DAF, this was of greater intensity and involved greater segments of glomeruli in *Daf*$^{-/-}$ and *Daf*$^{-/-}$*Cd59*$^{-/-}$ mice (Figure 1C).

Along with the marked albuminuria, *Daf*$^{-/-}$ and *Daf*$^{-/-}$*Cd59*$^{-/-}$ mice developed histological features of segmental sclerosis (representative photomicrographs from each group are shown in Figure 1D). The fractions of glomeruli involved with segmental sclerosis/hyalinosis were enumerated by a renal pathologist (M. Haas) masked to origin of slides (Figure 1E). As with albuminuria, the 4 groups were significantly different ($P < 0.002$). Thirteen of the 15 *Daf*$^{-/-}$ and *Daf*$^{-/-}$*Cd59*$^{-/-}$ mice developed FSGS, in which as much as 90% of glomeruli were involved, while only 3 of 15 WT and *Cd59*$^{-/-}$ mice developed FSGS, which affected at most 2% of glomeruli. Ultrastructural features of podocyte foot process effacement and injury along with prominent remodeling of the external side of the glomerular basement membrane were evident only in *Daf*$^{-/-}$ and *Daf*$^{-/-}$*Cd59*$^{-/-}$ mice (Figure 1F). Control WT and *Daf*$^{-/-}$ mice ($n = 3$ each group) given 0.67 mg/g body weight preimmune IgG (i.e., from the same sheep used to generate anti-podo Abs) failed to develop albuminuria above baseline or FSGS 30 days following injection.

Consistent with the belief that albuminuria predates and might even lead to pathological changes of FSGS, albuminuria measured at day 20 correlated strongly with FSGS scores 10 days later ($r = 0.69$; $P < 0.01$) and every animal with more than 3.0 mg urinary albumin/mg creatinine ($n = 14$) had histological FSGS 10 days later. In addition to urinary and histological features of FSGS, affected animals also developed hypoalbuminemia and hypercholesterolemia, classical biochemical features of the nephrotic syndrome. Thus, in WT, *Cd59*$^{-/-}$, *Daf*$^{-/-}$, and *Daf*$^{-/-}$*Cd59*$^{-/-}$ mice, respectively, serum albumin levels were 2.9 ± 0.2, 3.0 ± 0.2, 2.4 ± 0.1, and 2.2 ± 0.2 g/dl ($P < 0.01$, 1-way ANOVA), while serum cholesterol levels were 102.0 ± 1.1, 103.3 ± 4.6, 201.0 ± 10.3, and 182.0 ± 31.3 mg/dl ($P < 0.05$, 1-way ANOVA). These data from *Daf*$^{-/-}$ and *Daf*$^{-/-}$*Cd59*$^{-/-}$ mice differed little from each other but were significantly different from those of *Cd59*$^{-/-}$ and WT mice ($P < 0.05$ in all instances, Tukey's pairwise comparisons). In spite of these significant disease manifestations, there was no evidence for impaired glomerular filtration, with blood urea nitrogen (BUN) values from all animals at all times in the normal range (<30 mg/dl). Thus, disease induced by anti-podo Abs in DAF-deficient BALB/c mice has features characteristic of FSGS in humans.

Immunological events occurring in anti-podo Ab–induced FSGS. There were few infiltrating neutrophils or B cells but substantial accumulations of F4/80$^+$ monocytic and Thy-1.2$^+$ T cells in periglomerular locations (primarily surrounding focally sclerotic glomeruli) in DAF-deficient mouse kidneys given anti-podo Abs (Figure 2A); the quantities of both F4/80$^+$ monocytic and Thy-1.2$^+$ T cells were significantly higher than those in DAF-sufficient WT and *Cd59*$^{-/-}$ mice (Table 1). Using flow cytometry as an adjunctive approach to immunohistochemical enumeration of infiltrating cells, we found approximately 3 times more F4/80$^+$ cells than CD3$^+$ cells in DAF-deficient kidneys with FSGS; 75%–80% of the former were also CD11c$^+$ (Figure 2B), consistent with a DC phenotype that is also widely distributed in normal mouse kidneys (22). Thus, T cells and monocytic-type DCs significantly infiltrate the kidney in this experimental model of FSGS.

Given the findings of T cell accumulation and the fact that FSGS is considered to have a cellular immune basis, we evaluated T cell responses in vivo following sheep IgG administration. Initially, cellular proliferation was examined by incorporation of BrdU 10 days

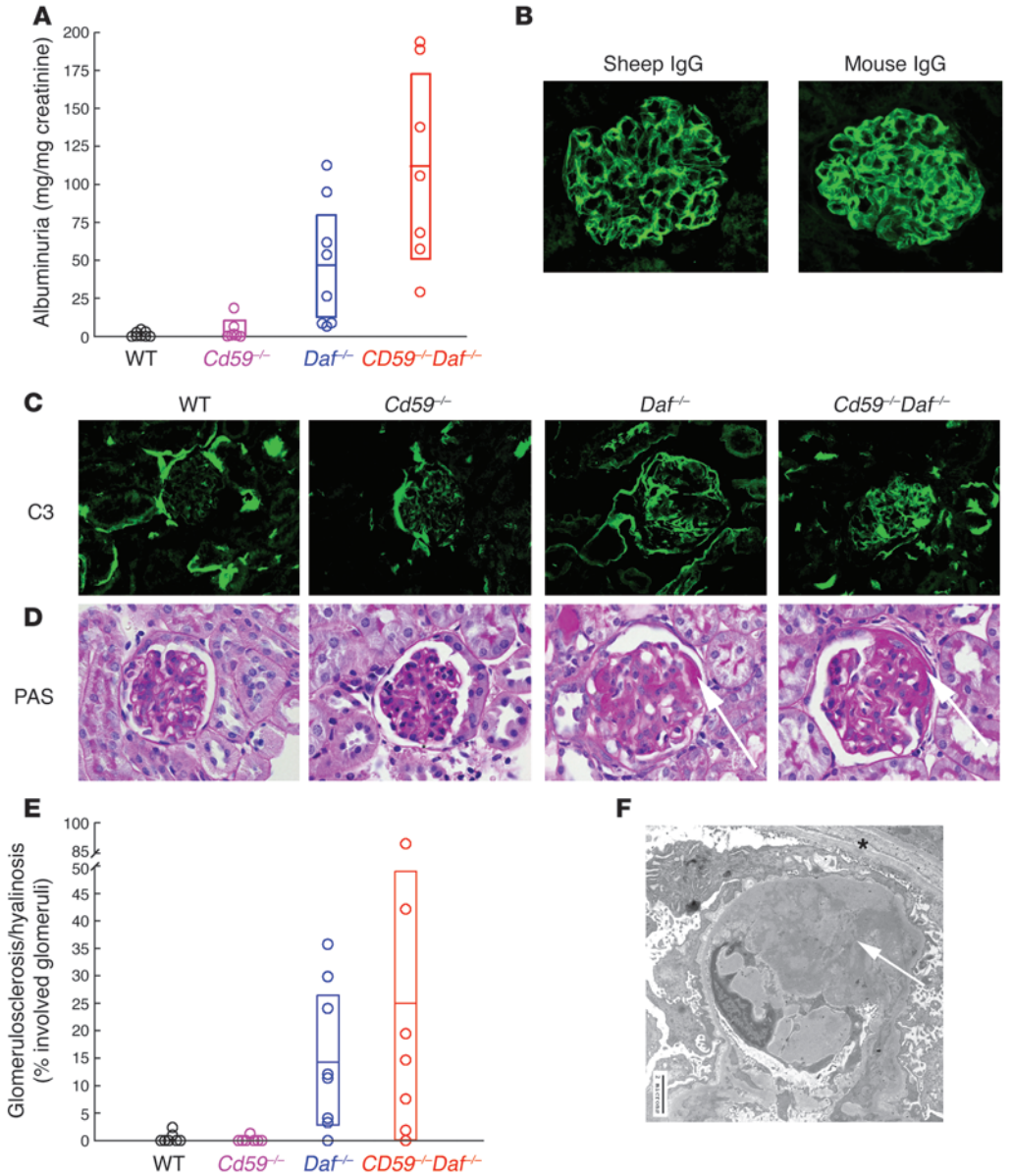

Figure 1

Anti-podo Ab–induced FSGS in DAF-deficient animals. (**A**) Significant albuminuria occurred in *Daf*$^{-/-}$ and *Cd59*$^{-/-}$*Daf*$^{-/-}$ mice 30 days after administration of anti-podo Abs. (**B**–**D**) Representative photomicrographs 30 days after anti-podo injection show glomerular localization of sheep and mouse IgG (**B**) and mouse C3 (**C**) in the 4 groups; (**D**) PAS-stained kidney sections show segmental sclerosis (arrows) only in *Daf*$^{-/-}$ and *Cd59*$^{-/-}$*Daf*$^{-/-}$ mice. (**E**) The extent of glomerulosclerosis in individual mice 30 days after administration of anti-podo Abs is shown. (**F**) Extensive podocyte foot process effacement and prominent remodeling of the external surface of the glomerular basement membrane (arrow) was seen by electron microscopy in DAF-deficient mice 30 days after anti-podo Abs administration. Asterisk denotes Bowman capsule. Numeric data shown in **A** and **E** from *Daf*$^{-/-}$ and *Daf*$^{-/-}$*Cd59*$^{-/-}$ mice were normally distributed, with means and 95% CIs shown as horizontal lines and open boxes, respectively. Data from WT and *Cd59*$^{-/-}$ mice were nonparametric (Anderson-Darling test; $P < 0.05$); when sufficiently different from the origin, the 95% CI for the median is shown as an open box. Original magnification, ×400 (**B**–**D**); ×7,100 (**F**).

after anti-podo IgG administration; in these studies, there were 1.30% ± 0.11% and 0.61% ± 0.21% BrdU$^+$ splenic CD4$^+$ cells in DAF-deficient and -sufficient hosts, respectively ($P < 0.01$, compared with that at day 0). Further analyses showed that DAF-deficient mice had greater activation of splenic CD4$^+$ cells compared with DAF-sufficient mice, as evidenced by the appearance and quantification of CD62L^{lo} and CD44^{hi} populations (Figure 2C and Table 2). This occurred in response to both preimmune and immune (i.e., anti-podo) IgG. The increased populations of CD62L^{lo}CD44^{hi} and BrdU$^+$ T cells in DAF-deficient mice exposed to sheep IgG is consistent with their having a heightened immune response that does not necessarily depend upon antigen localization (e.g., on or around podocytes) or potential downstream inflammatory events. To examine this in a more direct fashion, the appearance of sheep IgG on WT and DAF-deficient mouse PBMCs and splenocytes was evaluated after injection of nonimmune and anti-podo sheep IgG

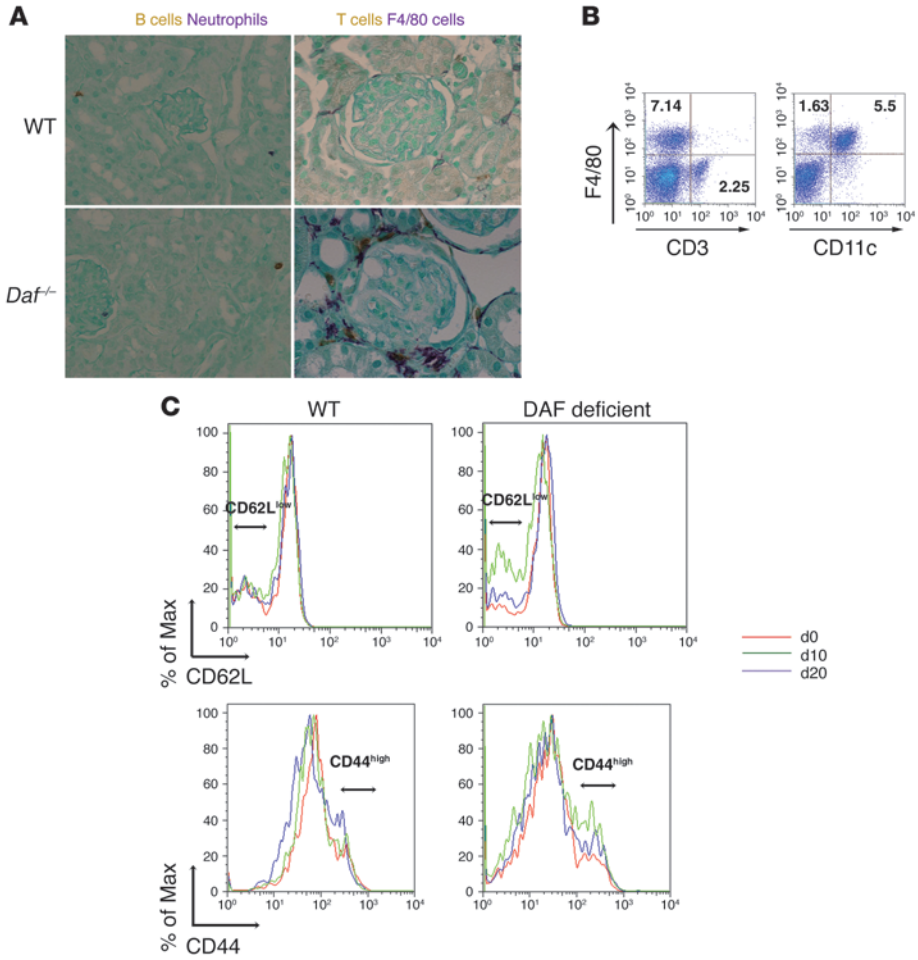

Figure 2
Immunological events induced by anti-podo Abs in DAF-deficient mice. (**A**) In the kidneys of all mice, there was little neutrophil (brown) or B cell (purple) infiltration, while in DAF-deficient mice, there was marked infiltration with Thy-1.2$^+$ T cells (brown) and F4/80$^+$ monocytic cells (purple). Original magnification, ×400. (**B**) Flow cytometric analysis of cells isolated from kidneys of DAF-deficient mice 30 days after anti-podo Ab administration showing relative proportions of F4/80$^+$ and CD3$^+$ cells (left panel). The majority of F4/80$^+$ cells were also CD11c$^+$ (right panel). Numbers shown are the percentage of total cells in individual quadrants. (**C**) Splenic CD4$^+$ cells from WT and DAF-deficient mice were assessed for CD62L (upper panels) and CD44 expression (lower panels) at baseline (d0) and 10 (d10) and 20 days (d20) after passive administration of anti-podo IgG. The CD62L^{lo} and CD44^{hi} populations are denoted by horizontal lines.

(Supplemental Figure 3). In all experimental combinations, sheep IgG was clearly evident on PBMCs within 4 hours of injection but declined in quantity such that 7 days after injection, there was no evident sheep IgG on PBMCs or splenocytes. On a quantitative basis, WT mice given anti-podo Abs had greater PBMC-associated sheep IgG compared with the other groups; since this group had the lowest specific immune response to sheep IgG (c.f., Table 2), this suggests the quantity of bound antigen does not translate directly into the level of immune response. Moreover, direct binding of anti-podo to immune cells does not appear to underlie the pathogenesis of this FSGS model.

Local renal versus systemic DAF deficiency. To evaluate the relative contributions of DAF within and outside the kidney, we transplanted WT kidneys into *Daf*$^{-/-}$ recipients, and *Daf*$^{-/-}$ kidneys into WT recipients (n = 7 each group). In this protocol, transplanted kidneys and their hosts were syngeneic other than at the *Daf1* gene. A single native nephrectomy was performed at the time of transplant. Following a 3-week recovery period, anti-podo Abs were administered to all animals. This approach allowed evaluation of 28 kidneys, equally divided among DAF-sufficient and -deficient donor and native kidneys. Surprisingly, the *Daf1* status of the kidney was unimportant in development of FSGS; instead, FSGS occurred only in those kidneys in which there was DAF deficiency outside the kidney. Thus, DAF-deficient kidneys and WT kidneys transplanted in *Daf*$^{-/-}$ recipients developed FSGS, while *Daf*$^{-/-}$ donor kidneys and WT native kidneys in WT hosts did not develop FSGS (Figure 3). Consistent with both kidneys developing FSGS in the DAF-deficient host was the urinary albumin excretion of 27.3 ± 14.0 and 0.4 ± 0.1 mg/mg creatinine in *Daf*$^{-/-}$ and *Daf*$^{+/+}$ (WT) hosts, respectively (P = 0.006). Furthermore, the extent of FSGS in donor WT kidneys was highly correlated with that in the native *Daf*$^{-/-}$ kidneys in the same mice (r = 0.99; P < 0.001). Thus, development of FSGS in this experimental model requires extrarenal DAF deficiency.

Relative roles for humoral and cellular immune systems in experimental FSGS. Given the apparent importance of T cell responses in the development of this Ab-induced FSGS model, we depleted CD4$^+$ cells in vivo using the mAb GK1.5 in *Daf*$^{-/-}$ mice starting 10 days after anti-podo administration; an isotype-matched irrelevant rat IgG_{2b} was used as control. On day 11, CD4$^+$ cells accounted for 0.09% ± 0.01% and 34.4% ± 2.7% of total circulating lymphocytes (P < 0.01), while at euthanasia on day 30, they were 5.5% ± 1.1% and 19.9% ± 0.7% of total splenic lymphocytes (P < 0.001) in GK1.5- and control mAb–treated mice, respectively. Thirty days after anti-podo Ab administration, each CD4$^+$ cell–depleted *Daf*$^{-/-}$ mouse had lower albuminuria and histological scores for FSGS than control animals (Figure 4A). Furthermore, CD4$^+$ cell depletion led to reduced renal infiltration with Thy1.2$^+$ (2.2 ± 0.0 versus 13.0 ± 1.2 cells/high-power field [hpf], P = 0.012) and F4/80$^+$ cells (38.1 ± 4.7 versus 61.2 ± 3.6 cells/hpf, P = 0.011) 30 days after anti-podo

Table 1
Accumulation of monocytic and T lymphocytic cells in kidneys of mice given anti-podo Abs

Cell	WT	*Cd59*$^{-/-}$	*Daf*$^{-/-}$	*Cd59*$^{-/-}$*Daf*$^{-/-}$
F4/80^{+A}	35.5 ± 2.8	49.2 ± 8.5	65.0 ± 6.5^{B}	95.3 ± 21.0^{B}
Thy-1.2^{+A}	4.7 ± 0.8	5.3 ± 0.5	15.3 ± 1.7^{B}	31.0 ± 12.5^{B}

Shown are cell numbers per renal cortical hpf. ^{A}The 4 groups had unequal variances ($P \leq 0.002$, 1-way ANOVA). $^{B}P < 0.02$ vs. WT and *CD59*$^{-/-}$ mice (Tukey's pairwise comparisons).

Ab injection (Figure 4B). This approach did not affect the *Daf*$^{-/-}$ mouse humoral immune response, at least as measured by total and isotype IgG anti-sheep IgG over time and glomerular IgG on day 30 (Supplemental Figure 4).

The collective data thus far showed that DAF deficiency outside the kidney and CD4^{+} cells were required for development of FSGS and that global DAF deficiency was associated with a heightened cellular immune response to sheep IgG. To further delineate the site where DAF deficiency was required, we first reconstituted T cell–deficient *Balb/c*$^{nu/nu}$ mice with enriched T cells from WT or *Daf*$^{-/-}$ mice. Because disease susceptibility tracked with DAF-deficient but not WT T cell preparations (discussed below), the possibility that other DAF-deficient cells (e.g., DCs) could have confounded these results was evaluated through further experiments using T cells highly purified by FACS. Lymphocytes were stably engrafted, and only those from WT donors expressed DAF (data not shown). In both sets of studies, *Balb/c*$^{nu/nu}$ mice with DAF-deficient T cells given anti-podo Abs developed significant albuminuria (Figure 4C) and increased renal infiltration with Thy1.2^{+} and F4/80^{+} cells (Table 3). In all but 1 mouse from each group given *Daf*$^{-/-}$ T cells, there was development of FSGS. Importantly, no mouse given partially or highly purified WT T cells developed abnormal albuminuria or FSGS (Figure 4, C and D).

BALB/c genetic background SCID mice, deficient in both B and T cells, were also reconstituted with flow cytometry–purified WT or *Daf*$^{-/-}$ T cells and given anti-podo Abs. Not unexpectedly, given the persistent absence of B cells, neither group generated anti-sheep IgG Abs; thus, while there was heterologous sheep IgG in glomeruli in the same intensity and patterns as in previous studies, there was no identifiable mouse IgG (data not shown). Surprisingly, SCID mice with DAF-deficient T cells developed a moderate degree of albuminuria, which was 30 times that of those receiving WT T cells, which was normal (1.0 ± 0.4 and 0.03 ± 0.01 mg albumin/mg creatinine, respectively; $P = 0.009$). However, no mouse in either group developed histological features of FSGS. These data indicate that the full FSGS disease model requires immune responses from both B and T cells, the latter necessarily DAF deficient.

Further investigations of the humoral immune response to sheep IgG were performed. As noted previously, glomeruli of all mice had marked deposition of mouse IgG in the glomerular capillary wall with no differences among groups. Yet titers of total IgG, and IgG_1 and IgG_{2a} anti-sheep IgG were lower in mice lacking DAF (*Daf*$^{-/-}$ and *Daf*$^{-/-}$*Cd59*$^{-/-}$) compared with those in mice that were DAF sufficient (WT and *Cd59*$^{-/-}$) (Figure 5A). To examine how DAF-deficient T cells fit into this observation, humoral responses of *Balb/c*$^{nu/nu}$ mice reconstituted with WT or *Daf*$^{-/-}$ T cells were also examined following anti-podo Ab administration. Interestingly, anti-sheep IgG, IgG_1, and IgG_{2a} titers were equivalent in both groups (Figure 5B). These data suggest that DAF deficiency outside T cells, including on B cells and DCs, leads to a relatively lower humoral immune response to sheep IgG, yet this did not affect the development of FSGS in this model.

Discussion

Here we report what we believe is a novel murine FSGS model that occurs in the autologous phase following passive transfer of anti-podo IgG Abs. Compared with previously established murine models of FSGS induced by reduction of renal mass (remnant kidney model) (23) or oxidative podocyte injury from systemic administration of puromycin aminonucleoside or adriamycin (24, 25), our model appears to be attributable to an adaptive cellular immune response to podocyte-bound heterologous IgG. This requires mice of BALB/c genetic background lacking the complement regulatory protein DAF. Other mouse strains, including DAF-deficient C57BL/6 mice, are totally resistant to this disease. Although the fundamental bases for these strain differences remain to be determined, that this is related to genetic background is highly likely. This is consistent with differing susceptibilities of inbred mouse strains to a variety of disease models (26, 27). For example, different patterns of nephrotoxic serum nephritis occur in C57BL/6 and BALB/c mice, which has been attributed to their respective Th1- and Th2-dominant immune responses (20, 28). Such a mechanism is believed to underlie other glomerulonephritis diseases modeled in the mouse as well as occurring in humans (29).

Our current model has features of human nephrotic syndrome, including progressive and severe albuminuria, hypoalbuminemia, and hypercholesterolemia. There were histological and ultrastructural features of podocyte injury, segmental glomerular sclerosis/hyalinosis, and periglomerular accumulations of T cells and monocytic cells. The latter were predominantly of DC origin, as evidenced by their bearing both F4/80 and CD11c proteins. Thus, this experimental model recapitulates features of FSGS in humans. Although there was evidence for tubulointerstitial inflammation, characteristic of proteinuric conditions regardless of underlying etiology (30), there was no impairment of renal excretory function, which is likely the consequence of our concentrating on the acute

Table 2
T cell responses to immune anti-podo and preimmune sheep IgG

Sheep IgG	WT mice			*Daf*$^{-/-}$ mice^{A}		
	d 0	d 10	d 20	d 0	d 10	d 20
Anti-podo Abs	8.5 ± 0.8	8.4 ± 0.8	7.6 ± 0.7	7.9 ± 0.7	10.5 ± 0.7	9.9 ± 0.5
Preimmune	8.0 ± 0.3	9.7 ± 1.8	9.5 ± 1.3	7.5 ± 1.2	13.0 ± 0.4	11.4 ± 1.4

Shown are percentages of CD4^{+} cells that were CD62L^{lo}CD44^{hi} before or 10 and 20 days after administration of anti-podo or preimmune sheep IgG. $^{A}P < 0.05$, comparing values before (day 0) and after (day 10 and day 20) administration of sheep IgG (as either preimmune or anti-podo IgG) (1-way ANOVA).

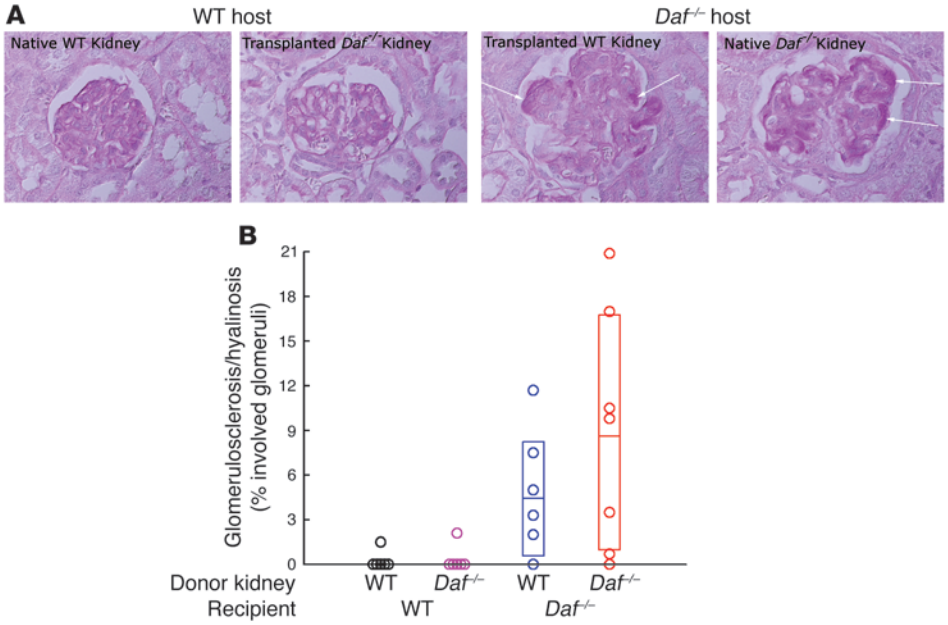

Figure 3
Kidney transplantation studies reveal extrarenal DAF deficiency is necessary for development of anti-podo Ab–induced FSGS. (**A**) Representative glomerular histopathology 30 days after anti-podo Ab administration in native WT and transplanted *Daf*$^{-/-}$ kidneys in a WT mouse and native *Daf*$^{-/-}$ and transplanted WT kidneys in a *Daf*$^{-/-}$ mouse. FSGS only developed in native and transplanted WT kidneys in *Daf*$^{-/-}$ mice. Arrows depict regions of segmental sclerosis/hyalinosis. Original magnification, ×400. (**B**) Shown is the extent of glomerulosclerosis in individual kidneys within each group. Data from native and transplanted kidneys in *Daf*$^{-/-}$ mice were normally distributed, while native and transplanted kidney data in WT mice were nonparametric (Anderson-Darling test; $P < 0.05$). Means and 95% CIs are shown as horizontal lines and open boxes, respectively.

phase of disease. Notably, Meyer et al. reported a passive anti-podo Ab model in mice in which Abs also located along podocytes and GBM (31). However, the pathological processes occurred mainly in the mesangial region and there was no sclerosis/fibrosis detected in any of these mice. Thus, the 2 models induced by injection of heterologous Abs to podocytes are clearly different. The development of FSGS in ours allowed us to delve into the fundamental immune bases underlying this important disease.

In this model, the development of anti-podo Ab–induced FSGS only occurred in DAF-deficient mice. Said differently, DAF prevented FSGS. The various disease features of FSGS only were present in DAF-deficient mice, whether or not they had the regulator of C5b-9 formation, CD59. While DAF-sufficient WT and *Cd59*$^{-/-}$ mice developed mild albuminuria (~5% that in DAF-deficient *Daf*$^{-/-}$ and *Daf*$^{-/-}$*Cd59*$^{-/-}$ mice), the development of FSGS was totally absent in these DAF-sufficient animals. Given its widespread distribution and key role in regulating complement activation (4, 32), DAF is protective in several experimental renal disease models, including nephrotoxic serum nephritis (5, 7), puromycin aminonucleoside nephrosis (33), chronic serum sickness (34), and renal ischemia/reperfusion injury (35). The mechanisms of the protection still need to be clarified, with mediators including C3a and C5a acting through their cognate receptors on intrinsic renal cells and/or extrinsic inflammatory cells. That CD59 appeared inconsequential in this model contrasts with other murine models, such as nephrotoxic serum nephritis (6) and renal ischemia/reperfusion (35), in which CD59 was relevant, thereby supporting a pathogenic role of C5b-9 formation on cells in renal pathology. These disease models occur when complement is activated by tissue-bound immune complexes formed by extrinsic or intrinsic (natural) Abs; particularly when DAF is not present to restrict C3 and C5 activation, C5b-9–mediated renal cellular injury can result. Our belief is that the present model of Ab-induced FSGS focuses cellular immunity to the site of complement activation, which is distinct from complement-mediated inflammation and/or direct tissue damage in other models of Ab-induced renal diseases.

Renal transplantation was used as a tool to determine the relative contribution of systemic and local (kidney) DAF deficiency in our model of FSGS. It was somewhat surprising that WT kidneys developed anti-podo Ab–induced FSGS when present in *Daf*$^{-/-}$ hosts, while *Daf*$^{-/-}$ kidneys in WT hosts were protected from developing FSGS. Furthermore, the extent of FSGS in the native *Daf*$^{-/-}$ and transplanted WT kidneys in the same *Daf*$^{-/-}$ host were significantly correlated. These data are strong evidence that extrarenal DAF deficiency dictates whether FSGS ensues or not, while local DAF deficiency is of considerably less consequence. Recurrence of proteinuria and primary disease in FSGS patients receiving normal donor kidneys occurs at a rate of 20% to 30% (36–38). A 30- to 50-kDa circulating molecule has been found to correlate with the recurrence of FSGS (16), though this has not been consistently shown in other studies (39). Thus, as with the transplant data from humans with FSGS, development of FSGS in our mouse model can be attributable to extrarenal factors. Whether there is a circulating "permeability factor" in this model as proposed in humans is the subject of our future studies.

The involvement of T cell immunity in patients with FSGS, and in particular a Th2-skewed response, has been suggested from cytokine profiles in affected patients (40, 41), yet there is little direct evidence for abnormal T cell immune responses in FSGS. In the current study, we used 2 approaches to assess T cells in FSGS. In vivo depletion of $CD4^+$ cells during the effector phase did not affect the humoral immune response to the passively transferred anti-podo Abs yet significantly reduced renal T cell and $F4/80^+$ cell accumulation and ameliorated albuminuria and FSGS in DAF-deficient mice. Adoptive transfer of *Daf*$^{-/-}$ T cells to T cell–deficient *Balb/c*$^{nu/nu}$ mice conferred susceptibility to FSGS, while *Balb/c*$^{nu/nu}$ mice reconstituted with WT T cells failed to develop FSGS. Similar results were obtained when highly purified T cells were used, which excluded potential APC/DC contamination in the transferred cells, adding strong support for the DAF-deficient T cell–dependent nature of this model. SCID mice that lacked B cells did not mount a humoral immune response to sheep IgG yet developed albuminuria but not FSGS when reconstituted with

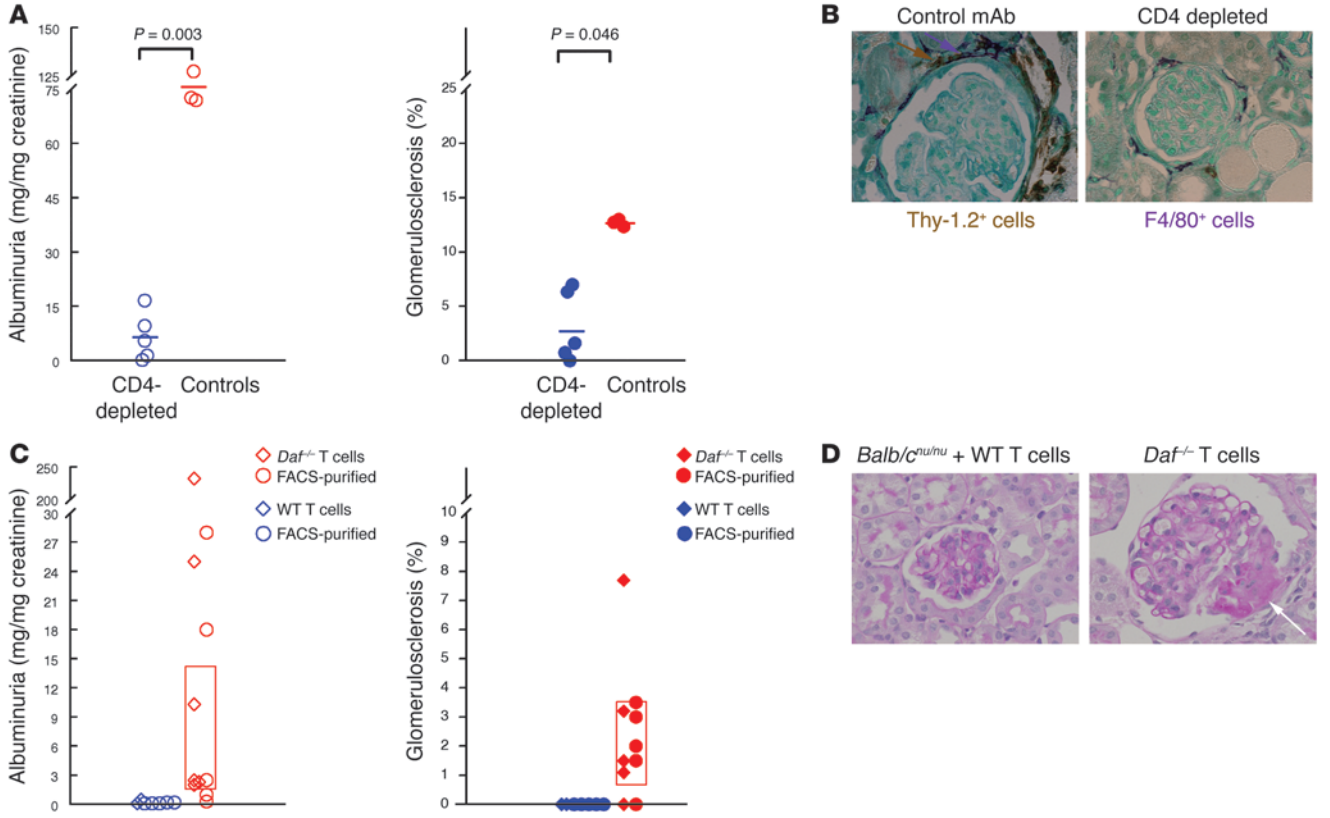

Figure 4

Susceptibility to anti-podo Ab–induced FSGS occurs when DAF is absent from T cells. (**A**) Shown are urinary albumin excretion (left) and the extent of glomerulosclerosis (right) 30 days after administration of anti-podo Abs in individual *Daf*$^{-/-}$ mice depleted of CD4$^+$ cells, with mAb GK1.5 or controls receiving irrelevant rat IgG_{2b}. All data were normally distributed (Anderson-Darling test; $P > 0.05$) and compared by *t* testing, with *P* values provided above the data. (**B**) Infiltration with Thy-1.2$^+$ T cells (brown, arrow) and F4/80$^+$ monocytic cells (purple, arrow) was significantly reduced 30 days after administration of anti-podo Abs in CD4$^+$ cell–depleted but not control *Daf*$^{-/-}$ mice. (**C**) *Balb/c*$^{nu/nu}$ mice reconstituted with DAF-deficient but not WT T cells developed albuminuria and FSGS. Urinary albumin excretion (left) and the percentage of segmentally sclerotic glomeruli (right) in individual *Balb/c*$^{nu/nu}$ mice that received T cells from WT (blue symbols) or *Daf*$^{-/-}$ mice (red symbols) 30 days after administration of anti-podo Abs. Experiments differed by whether mice were reconstituted with partially (diamonds) or highly (circles) purified T cells. All data sets in mice receiving T cells from *Daf*$^{-/-}$ mice were normally distributed with no differences comparing partially and highly purified T cells. Means and 95% CIs for the combined groups are shown as horizontal bars and open boxes, respectively. (**D**) Representative PAS-stained kidney sections from individual mice show the presence of segmental sclerosis (arrow) only in mice with DAF-deficient T cells. Original magnification, ×600.

DAF-deficient T cells. These data support the belief that FSGS, at least as modeled here, requires participation of host humoral immune responses as well as enhanced cellular immune responses by DAF-deficient T cells.

Recently, it has been shown that DAF has an important role in T cell immunity (13, 14). Deficiency of DAF significantly enhanced T cell responses in mice immunized with ovalbumin together with complete Freund's adjuvant, an effect that was dependent on complement and specifically C5a (13). Local complement alternative pathway activation facilitated by absent DAF on APCs is also essential to the hyperresponsiveness of T cells in *Daf*$^{-/-}$ mice (14). The functional significance of enhanced T cell responses in the setting of DAF deficiency was supported by the fact that *Daf*$^{-/-}$ mice had markedly enhanced disease development in the T cell–dependent experimental autoimmune encephalomyelitis model (13). Our present understanding of this still-unresolved topic is that DAF limits local generation of C3a/C5a, which provide important signals to APC/T cells (42, 43). It is also notable that DAF can provide a productive second signal to the primary one delivered through CD3, at least when cross-linked by fluid phase CD97 or anti-DAF Abs (9–12). In the current study, that enhanced T cellular immune responses were attributable to DAF deficiency was supported by the fact that *Daf*$^{-/-}$ mice had significantly higher CD4$^+$ T cell proliferation and increased numbers of CD4$^+$ effector memory (CD62L^{lo}CD44^{hi}) T cells after exposure to both preimmune and immune anti-podo sheep IgG.

Infiltration of kidneys, particularly around diseased glomeruli with F4/80$^+$ cells together with T cells is another important and interesting feature in this model. Renal F4/80$^+$ cells were initially referred to as resident macrophages (44). More recently, it has been determined that many of these renal F4/80$^+$ cells also express CD11c and/or CX_3CR1, consistent with a DC phenotype (45). Renal DCs form anatomic surveillance networks throughout the renal parenchyma, serving as sentinels under normal conditions in both mice and humans (45, 46). This surveillance function of renal DCs is supported by their ability to capture foreign antigen (22). Renal DCs can activate T cells, which can be further enhanced in the setting of local inflammation; this is not true

Table 3
Anti-podo Ab-induced renal infiltration with monocytic and T lymphocytic cells in *Balb/c*$^{nu/nu}$ mice reconstituted with WT or *Daf*$^{-/-}$ T cells

Cell	Enriched[A]		Sorted[B]	
	WT	*Daf*$^{-/-}$	WT	*Daf*$^{-/-}$
F4/80$^+$	14.6 ± 2.7	28.8 ± 3.4[C]	7.7 ± 0.6	13.9 ± 2.1[C]
Thy-1.2$^+$	1.3 ± 0.2	5.3 ± 1.0[C]	1.8 ± 0.1	3.1 ± 0.4[C]

Shown are cell numbers per renal cortical hpf. [A]More than 85% T cells. [B]More than 99% T cells. [C]$P \leq 0.03$ vs. WT, 2-sample *t* test.

for splenic DC activation, indicating a specificity to local renal DC surveillance (45). Accumulation of F4/80$^+$ cells in disease sites has been found in different renal disease models, such as lupus nephritis (47), nephrotoxic serum nephritis (48), unilateral ureteral obstruction (49, 50), and ischemia/reperfusion injury (51), indicating their abilities to react to myriad renal insults. In the current study, the accumulation of F4/80$^+$CD11c$^+$ monocytic/DCs and Thy-1.2$^+$CD3$^+$ T cells was evident only in *Daf*$^{-/-}$ mice. These findings suggest an active role for DCs and T cells in the kidney and their functional connections in the development of this experimental FSGS model.

Our current study provides evidence of an Ab-induced glomerular injury model in relatively Th2-skewed BALB/c mice. When T cells lack DAF, a model recapitulating functional and structural features of human FSGS ensues. Enhanced T cell responses to sheep IgG "planted" on podocytes and accumulation of monocytic/DCs and T cells around diseased glomeruli were evident only in DAF-deficient mice. DAF-deficient kidneys were protected from FSGS when present in a DAF-sufficient host, indicating that key pathophysiological factor(s) of this disease reside outside the kidney. The fact that depletion of CD4$^+$ cells prevented *Daf*$^{-/-}$ mice from developing FSGS and *Balb/c*$^{nu/nu}$ mice reconstituted with *Daf*$^{-/-}$ T cells but not WT T cells developed FSGS firmly implicates an enhanced cellular immune response as critical in the development of FSGS in this model.

Methods

Animals. Mice with targeted deletions of *Daf1* and *Cd59a* were generated as described previously (7, 52) and were backcrossed onto the BALB/c background for at least 10 generations. Homozygous *Daf1*$^{-/-}$ and *Cd59a*$^{-/-}$ mice were generated by intercrossing heterozygous mice and screened by flow cytometry as described (32, 52). Doubly DAF- and CD59-deficient mice were generated by intercrossing *Daf1*$^{-/-}$ and *Cd59a*$^{-/-}$ mice. T cell–deficient nude mice on a BALB/c background (*CAnN.Cg-Foxn1*^{nu}*/Crl*) and WT BALB/c mice were purchased from Charles River. T cell– and B cell–deficient mice on a BALB/c background (*CBySmn.CB17-Prkdc*^{scid}/J) were purchased from The Jackson Laboratory. All studies were performed on animals between the ages of 10 and 12 weeks, followed the NIH Guide for the Care and Use of Laboratory Animals, and were approved by the University of Chicago Animal Care and Use Committee.

Sheep were hyperimmunized with proteins isolated from cultured mouse podocytes. Serum isolated at one time from an individual sheep was used to generate anti-podo IgG. In initial dosing studies, *Daf*$^{-/-}$ *Cd59*$^{-/-}$ mice received a single i.p. injection of 0, 0.17, 0.33, or 0.67 mg/g body weight anti-podo Abs ($n \geq 2$ per group). Five days following Ab injection, renal biopsies were performed on 1 mouse from each group. Blood and urine samples were collected from all animals 5, 10, 20, and 30 days following anti-podo Ab administration, and mice were euthanized at the latter time point.

Based on these pilot studies, we concentrated on events 30 days after 0.67 mg/g body weight anti-podo IgG administration in WT ($n = 8$), *Cd59*$^{-/-}$ ($n = 7$), *Daf*$^{-/-}$ ($n = 8$), and *Cd59*$^{-/-}$*Daf*$^{-/-}$ ($n = 7$) mice. As controls, equal amounts of preimmune sheep IgG were also given to WT and *Daf*$^{-/-}$ mice ($n = 3$ in each group). To characterize earlier disease features, other groups of mice were euthanized 10 or 20 days after anti-podo or preimmune sheep IgG administration. Binding of anti-podo Abs within glomeruli as well as potential binding to PBMCs and splenocytes was evaluated by immunoelectron microscopy and flow cytometry for sheep IgG, respectively, for varying times after anti-podo Ab injection.

Kidney transplantation was performed in a separate group of mice. The transplantation surgery was performed as described earlier (53). In brief, donor mice were anesthetized and the donor left kidney was removed with artery, vein, and ureter attached and preserved in cold saline on ice. The recipient was then anesthetized, and the left kidney was excised. End-to-side anastomoses of the donor renal vein, artery, and ureter to the recipient inferior vena cava, aorta, and bladder, respectively, were performed. Kidney transplantations were performed between *Daf*$^{-/-}$ and WT mice ($n = 7$ per group, with each animal serving as donor or recipient). Mice were allowed to recover from transplantation for 3 weeks, after which time renal function was normal. Transplanted mice received 0.67 mg/g body weight anti-podo Abs, followed 30 days later by euthanasia and harvesting of native and transplanted kidneys.

In a separate group of *Daf*$^{-/-}$ mice ($n = 5$) receiving anti-podo Abs, animals were given 0.2 mg anti-CD4 mAbs (clone GK1.5, provided by Yangxin Fu, University of Chicago) 10 and 17 days after anti-podo administration; such an approach has been documented to effectively deplete CD4$^+$ cells over the period of interest for these studies (54). Control mice received 0.2 mg isotype-matched rat IgG_{2b} (AbD Serotec) on the same schedule. One day after each mAb treatment, peripheral CD4$^+$ cell populations were examined by flow cytometry (FACSCanto; BD Biosciences) using anti-CD4 mAb clone RM4-5 (BD Biosciences — Pharmingen). At euthanasia 30 days after anti-podo Ab administration (and 13 days following the last GK1.5 dose), peripheral and splenic CD4$^+$ cells were also analyzed by flow cytometry.

To dissect the role of DAF on T cells, adoptive transfers of T cells were performed as described by others (55). In brief, spleens from *Daf*$^{-/-}$ mice or WT BALB/c mice were minced, erythrocytes were lysed with NH_4Cl, and the cell suspension was passed through a 40-μm cell strainer (BD Biosciences). Enriched T cells (>85% pure) were obtained using mouse T cell enrichment columns (R&D Systems) following the manufacturer's instructions. To generate highly purified T cells (>99% pure), isolated splenocytes were incubated with PE-conjugated rat anti-mouse Thy1.2 (BD Biosciences). Thy1.2$^+$ cells were sorted using a MoFlo Cell Sorter (Beckman Coulter). Approximately 1.5×10^7 enriched *Daf*$^{-/-}$ ($n = 5$) or WT ($n = 2$) T cells were injected i.v. into *Balb/c*$^{nu/nu}$ mice, while approximately 1.2×10^7 purified *Daf*$^{-/-}$ or WT T cells were injected i.v. into *Balb/c*$^{nu/nu}$ or B cell– and T cell–deficient *Balb/c*^{scid} mice ($n = 5$ per each of the 4 conditions). The injected T cells were allowed to reconstitute for 4 weeks (56), after which mice received 0.67 mg/g body weight anti-podo Abs.

Measurements from serum and urine. Blood urea nitrogen (BUN) concentrations were detected with a Beckman Autoanalyzer (Beckman Coulter). Serum albumin and cholesterol concentrations were determined with an Olympus AU400 analyzer (Olympus). Urinary albumin concentrations were measured with a mouse albumin ELISA kit (Bethyl Laboratories Inc.) and normalized to creatinine concentrations in the same urine (measured with Stanbio Creatinine Procedure No. 0400; Stanbio Laboratory) as described previously (57).

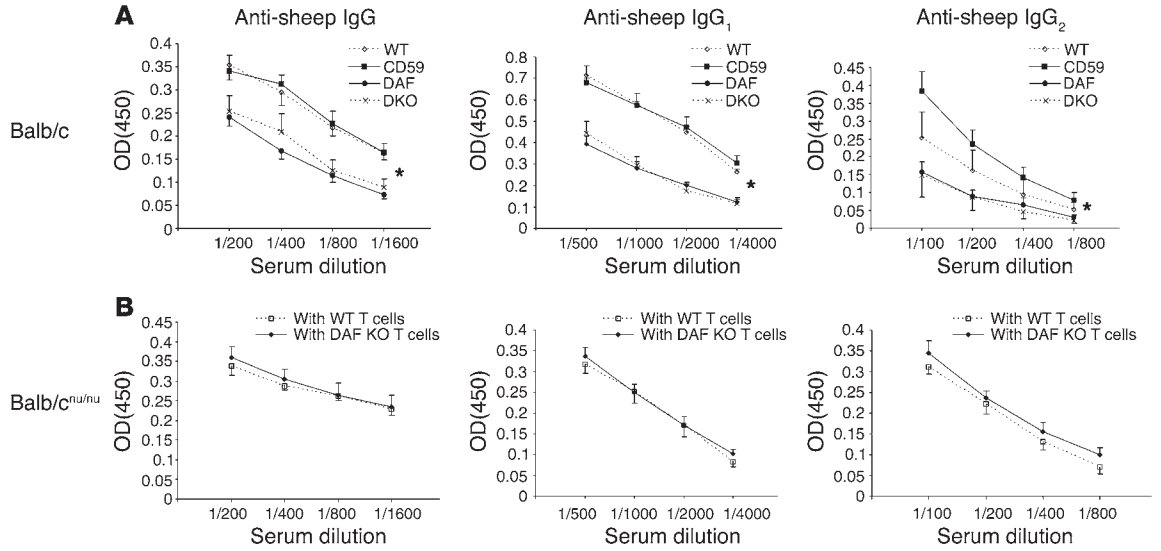

Figure 5

Abnormal anti-sheep IgG responses occur when DAF is absent outside T cells. (**A**) Serum mouse IgG, IgG_1, and IgG_{2a} anti-sheep IgG titers were higher in WT (open diamonds) and *Cd59*$^{-/-}$ mice (filled squares) compared with *Daf*$^{-/-}$ (filled circles) and *Cd59*$^{-/-}$*Daf*$^{-/-}$ (X's) mice. *$P < 0.01$, IgG concentration in DAF-sufficient versus DAF-deficient mice. (**B**) *Balb/c*$^{nu/nu}$ mice reconstituted with T cells from *Daf*$^{-/-}$ (filled diamonds) or WT mice (open squares) had comparable serum titers of mouse IgG, IgG_1, and IgG_{2a} anti-sheep IgG. Data shown represent mean ± SEM.

Measurements from renal tissue. To evaluate renal pathological changes, kidney tissues were fixed in 4% paraformaldehyde and embedded in paraffin. 3-μm sections were stained with PAS and examined by a renal pathologist (M. Haas) masked to the origin of the slides. The number of glomeruli with segmental sclerosis and/or hyalinosis was determined and expressed as a percentage of total glomeruli observed in the entire cortical field. For immunofluorescence microscopy, 4-μm cryostat sections were fixed in ether-ethanol and stained with FITC-conjugated antibodies to mouse C3, mouse IgG (Cappel Pharmaceuticals Inc.), or sheep IgG (Sigma-Aldrich). The glomerular distribution and semiquantitative score of staining intensity (from 0 to 4) was compiled in a masked manner as described previously (57). To observe potential ultrastructural changes induced by anti-podo Abs, renal cortical tissues randomly selected from each group of mice were processed and evaluated by electron microscopy by a renal pathologist (C. Alpers) using standard techniques (57).

To evaluate the composition of renal cellular infiltrates, immunohistochemistry was performed on 4% paraformaldehyde-fixed and paraffin-embedded kidney sections. Endogenous peroxidases and biotin were blocked by 0.3% hydrogen peroxide and Avidin/Biotin Blocking Kit (Vector Laboratories), with 10% normal goat serum used as a separate blocking step. The slides were then incubated with rat anti-mouse Ly-6G (Cell Sciences) for neutrophils, anti-B220 (BD Biosciences — Pharmingen) for B cells, anti–Thy-1.2 (AbD Serotec) for T cells, and anti-F4/80 (AbD Serotec) for monocytic cells, followed by goat anti-rat IgG (BD Biosciences — Pharmingen) and streptavidin-peroxidase (Sigma-Aldrich). Specifically bound Abs were detected by DAB Substrate Kit (Vector Laboratories). To quantify each cell type within renal cortices, at least twenty ×400 fields were examined by an observer masked to origin of the slides. To compare the distribution of different inflammatory cell types, double immunohistochemistry staining was performed. Slides were first stained with rat anti-mouse Thy-1.2 or anti-mouse B220 as described above. The specific Ab binding was detected by DAB development. The peroxidases and biotin in the first staining were blocked by 0.3% hydrogen peroxide and Avidin/Biotin Blocking Kit. Then the slides were incubated with rat anti-F4/80 or anti–Ly-6G as described above. Specific signal was detected by VIP Substrate Kit (Vector Laboratories). Finally, the sections were counterstained with Methyl Green (Vector Laboratories).

Flow cytometry of renal cells. We used a protocol adapted from previously published methods to isolate cells from kidneys (45). In brief, mouse kidneys were minced into very fine pieces and digested at 37°C for 45 minutes with gentle agitation with collagenase I (2 mg/ml) and DNAse I (100 μg/ml) in HBSS/1% (v/v) BSA (all from Sigma-Aldrich). Erythrocytes were lysed with NH_4Cl, and the cell suspension was passed through a 40-μm cell strainer (BD Biosciences), followed by density centrifugation through NycoPrep 1.077A (Axis-Shield). Isolated cells (~10^6) from each mouse were stained with F4/80-FITC (AbD Serotec), CD3-PECy5, and CD11c-PECy7 (BD Biosciences — Pharmingen). Flow cytometry was performed with a FACSCanto (BD Biosciences) and analyzed with FlowJo software, version 8 (Tree Star).

Assessments of immunological activity. For detection of circulating mouse anti-sheep IgG, IgG_1, and IgG_{2a}, 96-well plates were coated with 5 μg/ml sheep IgG. After blocking with 1% BSA, plates were incubated with serial dilutions of sera, followed by HRP-conjugated anti-mouse IgG (Jackson ImmunoResearch Laboratories Inc.) or HRP-conjugated anti-mouse IgG_1 or IgG_{2a} (AbD Serotec). Specific binding was detected using *o*-phenylenediamine as substrate (Sigma-Aldrich) followed by measurement of OD_{450} in a microtiter plate reader (BioTek). Sera from normal unmanipulated WT mice and those immunized with anti-podo Abs were used as negative and positive controls in all plates. Extrapolated values (U/ml) for each mouse relative to these controls were generated in triplicate, which allowed accurate statistical comparisons among groups.

The subsets and the activation status of lymphocytes were determined. *Daf*$^{-/-}$ and WT mice received anti-podo Ab IgG, nonimmune sheep IgG, or saline (n = 3–4 per group). Incorporation of BrdU (BD Biosciences — Pharmingen) in vivo was used to evaluate T cell proliferation. Seven or 17 days after administration of anti-podo or preimmune IgG, these mice as well as further controls not injected with sheep IgG were given 1 mg BrdU i.p. daily for 3 days. Splenocytes (~10^6 cells) were isolated as described above and stained for the following cell surface markers (in varying combi-

nations, with the label in parentheses; all from BD Biosciences — Pharmingen): B220 (FITC), CD3 (PE-Cy5), CD4 (allophycocyanin), CD8 (PE-Cy7), CD44 (PE), and CD62L (FITC). Intracellular staining of incorporated BrdU was performed using a standard kit according to the manufacturer's instructions (BD Biosciences — Pharmingen). Flow cytometry was then performed and analyzed as described above.

Statistics. Numeric data from all experiments were first analyzed using the graphical summary function in Minitab 15, which allowed determination of data normality (Anderson-Darling test) and 95% CIs for mean, median, and standard deviations. For some data sets, these fundamental properties were graphically depicted. Parametric and nonparametric data were then analyzed by 1-way ANOVA and Kruskal-Wallis tests, respectively. When data sets were significantly different by these measures, subsequent comparisons were made by Tukey's testing and sign CIs for parametric and nonparametric data, respectively; appropriate corrections for multiple comparisons were always incorporated in these analyses. When only 2 groups of data were generated in a given experiment, 2-sample *t* test and Mann-Whitney tests were used for parametric and nonparametric data, respectively. To determine whether a normally distributed data sample deviated from zero, a 1-sided/1-sample *t* test was used. To analyze potential correlations among data sets, Pearson product moment correlation coefficients and associated *P* values were calculated. $P < 0.05$ was considered significant.

Acknowledgments

We thank Yang-Xin Fu (University of Chicago) for supplying GK1.5 Ab. This work was supported by NIH R01 grants: DK041873 and DK055357 (to R.J. Quigg); DK051096 and DK056799 (to S.J. Shankland); AI044970, AI049344, and AI063288 (to W.-C. Song); DK066802 (to C.E. Alpers); and AR049775 (to J. Zhang).

Received for publication April 22, 2008, and accepted in revised form February 10, 2009.

Address correspondence to: Lihua Bao or Richard J. Quigg, Section of Nephrology, University of Chicago, 5841 S. Maryland Ave., MC5100, Chicago, Illinois 60637, USA. Phone: (773) 834-7480; Fax: (773) 702-5818; E-mail: lbao@medicine.bsd.uchicago.edu (L. Bao). Phone: (773) 702-0757; Fax: (773) 702-4816; E-mail: rquigg@medicine.bsd.uchicago.edu (R.J. Quigg).

1. Walport, M.J. 2001. Advances in immunology: complement (first of two parts). *N. Engl. J. Med.* **344**:1058–1066.
2. Speth, C., Prodinger, W.M., Würzner, R., Stoibert, H., and Dierich, M.P. 1993. Complement. In *Fundamental immunology*. 6th edition. W.E. Paul, editor. Lippincott Williams & Wilkins. Baltimore, Maryland, USA. 1047–1078.
3. Holers, V.M. 2001. Complement deficiencies. In *Clinical immunology: principles and practice*. 2nd edition. R. Rich, editor. Mosby. St. Louis, Missouri, USA. 36.1–36.10.
4. Harris, C.L., Rushmere, N.K., and Morgan, B.P. 1999. Molecular and functional analysis of mouse decay accelerating factor (CD55). *Biochem. J.* **341**:821–829.
5. Lin, F., Emancipator, S.N., Salant, D.J., and Medof, M.E. 2002. Decay-accelerating factor confers protection against complement- mediated podocyte injury in acute nephrotoxic nephritis. *Lab. Invest.* **82**:563–569.
6. Lin, F., et al. 2004. Respective roles of decay-accelerating factor and CD59 in circumventing glomerular injury in acute nephrotoxic serum nephritis. *J. Immunol.* **172**:2636–2642.
7. Sogabe, H., et al. 2001. Increased susceptibility of decay-accelerating factor deficient mice to anti-glomerular basement membrane glomerulonephritis. *J. Immunol.* **167**:2791–2797.
8. O'Brien, D.P., et al. 2006. The role of decay-accelerating factor as a receptor for Helicobacter pylori and a mediator of gastric inflammation. *J. Biol. Chem.* **281**:13317–13323.
9. Davis, L.S., Patel, S.S., Atkinson, J.P., and Lipsky, P.E. 1988. Decay-accelerating factor functions as a signal transducing molecule for human T cells. *J. Immunol.* **141**:2246–2252.
10. Shenoy-Scaria, A.M., et al. 1992. Signal transduction through decay-accelerating factor: Interaction of glycosyl-phosphatidylinositol anchor and protein tyrosine kinases $p56^{lck}$ and $p59^{fyn\ 1}$. *J. Immunol.* **149**:3535–3541.
11. Hamann, J., Vogel, B., van Schijndel, G.M., and van Lier, R.A. 1996. The seven-span transmembrane receptor CD97 has a cellular ligand (CD55, DAF). *J. Exp. Med.* **184**:1185–1189.
12. Qian, Y.M., Haino, M., Kelly, K., and Song, W.C. 1999. Structural characterization of mouse CD97 and study of its specific interaction with the murine decay-accelerating factor (DAF, CD55). *Immunology.* **98**:303–311.
13. Liu, J., et al. 2005. The complement inhibitory protein DAF (CD55) suppresses T cell immunity in vivo. *J. Exp. Med.* **201**:567–577.
14. Heeger, P.S., et al. 2005. Decay-accelerating factor modulates induction of T cell immunity. *J. Exp. Med.* **201**:1523–1530.
15. Shankland, S.J. 2006. The podocyte's response to injury: role in proteinuria and glomerulosclerosis. *Kidney Int.* **69**:2131–2147.
16. Savin, V.J., et al. 1996. Circulating factor associated with increased glomerular permeability to albumin in recurrent focal segmental glomerulosclerosis. *N. Engl. J Med.* **334**:878–883.
17. Quigg, R.J., et al. 1989. Studies with antibodies to cultured rat glomerular epithelial cells: Subepithelial immune deposit formation after in vivo injection. *Am. J. Pathol.* **134**:1125–1133.
18. Lin, F., et al. 2001. Tissue distribution of products of the mouse decay-accelerating factor (DAF) genes. Exploitation of a Daf1 knock-out mouse and site-specific monoclonal antibodies. *Immunology.* **104**:215–225.
19. Quigg, R.J., Nicholson-Weller, A., Cybulsky, A.V., Badalamenti, J., and Salant, D.J. 1989. Decay accelerating factor regulates complement activation on glomerular epithelial cells. *J. Immunol.* **142**:877–882.
20. Huang, X.R., Holdsworth, S.R., and Tipping, P.G. 1997. Th2 responses induce humorally mediated injury in experimental anti-glomerular basement membrane glomerulonephritis. *J. Am. Soc. Nephrol.* **8**:1101–1108.
21. Chen, J.S., et al. 2006. Mouse model of membranous nephropathy induced by cationic bovine serum albumin: antigen dose-response relations and strain differences. *Nephrol. Dial. Transplant.* **19**:2721–2728.
22. Soos, T.J., et al. 2006. CX3CR1+ interstitial dendritic cells form a contiguous network throughout the entire kidney. *Kidney Int.* **70**:591–596.
23. Ma, L.J., and Fogo, A.B. 2003. Model of robust induction of glomerulosclerosis in mice: importance of genetic background. *Kidney Int.* **64**:350–355.
24. Diamond, J.R., Bonventre, J.V., and Karnovsky, M.J. 1986. A role for oxygen free radicals in aminonucleoside nephrosis. *Kidney Int.* **29**:478–483.
25. Kawaguchi, M., Yamada, M., Wada, H., and Okigaki, T. 1992. Roles of active oxygen species in glomerular epithelial cell injury in vitro caused by puromycin aminonucleoside. *Toxicology.* **72**:329–340.
26. Qi, Z., et al. 2005. Characterization of susceptibility of inbred mouse strains to diabetic nephropathy. *Diabetes.* **54**:2628–2637.
27. He, C., et al. 1996. Dissociation of glomerular hypertrophy, cell proliferation, and glomerulosclerosis in mouse strains heterozygous for a mutation (Os) which induces a 50% reduction in nephron number. *J. Clin. Invest.* **97**:1242–1249.
28. Huang, X.R., Tipping, P.G., Shuo, L., and Holdsworth, S.R. 1997. Th1 responsiveness to nephritogenic antigens determines susceptibility to crescentic glomerulonephritis in mice. *Kidney Int.* **51**:94–103.
29. Holdsworth, S.R., Kitching, A.R., and Tipping, P.G. 1999. Th1 and Th2 T helper cell subsets affect patterns of injury and outcomes in glomerulonephritis. *Kidney Int.* **55**:1198–1216.
30. Ruggenenti, P., and Remuzzi, G. 2000. The role of protein traffic in the progression of renal diseases. *Annu. Rev. Med.* **51**:315–327.
31. Meyer, T.N., et al. 2007. A new mouse model of immune-mediated podocyte injury. *Kidney Int.* **72**:841–852.
32. Miwa, T., et al. 2001. Characterization of glycosylphosphatidylinositol-anchored decay accelerating factor (GPI-DAF) and transmembrane DAF gene expression in wild-type and GPI-DAF gene knockout mice using polyclonal and monoclonal antibodies with dual or single specificity. *Immunology.* **104**:207–214.
33. Bao, L., et al. 2002. Decay-accelerating factor expression in the rat kidney is restricted to the apical surface of podocytes. *Kidney Int.* **62**:2010–2021.
34. Bao, L., Haas, M., Minto, A.W., and Quigg, R.J. 2007. Decay-accelerating factor but not CD59 limits experimental immune-complex glomerulonephritis. *Lab. Invest.* **87**:357–364.
35. Yamada, K., Miwa, T., Liu, J., Nangaku, M., and Song, W.C. 2004. Critical protection from renal ischemia reperfusion injury by CD55 and CD59. *J. Immunol.* **172**:3869–3875.
36. Pinto, J., et al. 1981. Recurrence of focal segmental glomerulosclerosis in renal allografts. *Transplantation.* **32**:83–89.
37. Senggutuvan, P., et al. 1990. Recurrence of focal segmental glomerulosclerosis in transplanted kidneys: analysis of incidence and risk factors in 59 allografts. *Pediatr. Nephrol.* **4**:21–28.
38. Hubsch, H., et al. 2005. Recurrent focal glomerulosclerosis in pediatric renal allografts: the Miami experience. *Pediatr. Nephrol.* **20**:210–216.
39. Godfrin, Y., et al. 1997. Study of the in vitro effect

on glomerular albumin permselectivity of serum before and after renal transplantation in focal segmental glomerulosclerosis. *Transplantation.* **64**:1711–1715.
40. Neuhaus, T.J., Wadhwa, M., Callard, R., and Barratt, T.M. 1995. Increased IL-2, IL-4 and interferon-gamma (IFN-gamma) in steroid-sensitive nephrotic syndrome. *Clin. Exp. Immunol.* **100**:475–479.
41. Yap, H.K., et al. 1999. Th1 and Th2 cytokine mRNA profiles in childhood nephrotic syndrome: evidence for increased IL-13 mRNA expression in relapse. *J. Am. Soc. Nephrol.* **10**:529–537.
42. Liu, J., et al. 2008. IFN-gamma and IL-17 production in experimental autoimmune encephalomyelitis depends on local APC-T cell complement production. *J. Immunol.* **180**:5882–5889.
43. Strainic, M.G., et al. 2008. Locally produced complement fragments C5a and C3a provide both costimulatory and survival signals to naive CD4+ T cells. *Immunity.* **28**:425–435.
44. Hume, D.A., Robinson, A.P., MacPherson, G.G., and Gordon, S. 1983. The mononuclear phagocyte system of the mouse defined by immunohistochemical localization of antigen F4/80. Relationship between macrophages, Langerhans cells, reticular cells, and dendritic cells in lymphoid and hematopoietic organs. *J. Exp. Med.* **158**:1522–1536.
45. Kruger, T., et al. 2004. Identification and functional characterization of dendritic cells in the healthy murine kidney and in experimental glomerulonephritis. *J. Am. Soc. Nephrol.* **15**:613–621.
46. Woltman, A.M., et al. 2007. Quantification of dendritic cell subsets in human renal tissue under normal and pathological conditions. *Kidney Int.* **71**:1001–1008.
47. Patole, P.S., et al. 2006. Expression and regulation of Toll-like receptors in lupus-like immune complex glomerulonephritis of MRL-Fas(lpr) mice. *Nephrol. Dial. Transplant.* **21**:3062–3073.
48. Masaki, T., Chow, F., Nikolic-Paterson, D.J., Atkins, R.C., and Tesch, G.H. 2003. Heterogeneity of antigen expression explains controversy over glomerular macrophage accumulation in mouse glomerulonephritis. *Nephrol. Dial. Transplant.* **18**:178–181.
49. Yoo, K.H., et al. 2006. Osteopontin regulates renal apoptosis and interstitial fibrosis in neonatal chronic unilateral ureteral obstruction. *Kidney Int.* **70**:1735–1741.
50. Kitagawa, K., et al. 2004. Blockade of CCR2 ameliorates progressive fibrosis in kidney. *Am. J. Pathol.* **165**:237–246.
51. Dong, X., et al. 2007. Resident dendritic cells are the predominant TNF-secreting cell in early renal ischemia-reperfusion injury. *Kidney Int.* **71**:619–628.
52. Miwa, T., Zhou, L., Hilliard, B., Molina, H., and Song, W.C. 2002. Crry, but not CD59 and DAF, is indispensable for murine erythrocyte protection in vivo from spontaneous complement attack. *Blood.* **99**:3707–3716.
53. Cunningham, P.N., Wang, Y., Guo, R., He, G., and Quigg, R.J. 2004. Role of Toll-like receptor 4 in endotoxin-induced acute renal failure. *J. Immunol.* **172**:2629–2635.
54. Yu, P., et al. 2004. Priming of naive T cells inside tumors leads to eradication of established tumors. *Nat. Immunol.* **5**:141–149.
55. Rabb, H., et al. 2000. Pathophysiological role of T lymphocytes in renal ischemia-reperfusion injury in mice. *Am. J. Physiol. Renal Physiol.* **279**:F525–F531.
56. Burne, M.J., et al. 2001. Identification of the CD4(+) T cell as a major pathogenic factor in ischemic acute renal failure. *J. Clin. Invest.* **108**:1283–1290.
57. Quigg, R.J., et al. 1998. Immune complex glomerulonephritis in C4- and C3-deficient mice. *Kidney Int.* **53**:320–330.